SOIL AMPLIFICATION IN PROBABILISTIC GROUND MOTION HAZARD ANALYSIS

S. Barani[1] (barani@dipteris.unige.it) and D. Spallarossa[1]

[1]Dipartimento di Scienze della Terra dell'Ambiente e della Vita, Università di Genova, Italy

Abstract

The article presents a comparison of different probabilistic methods for ground motion hazard assessments that include site effects. The approaches examined here were selected and refined during the different phases of the S2-Project, which this journal volume is addressed to. Different procedures characterized by different levels of sophistication, from the simpler one based on the use of standard ground motion predictive equations for specific ground types to the more complex one based on the convolution of a site-specific amplification function (and its variability) with the hazard curve for reference rock, are compared and contrasted with the aim of pointing out strengths and weaknesses of each of them. In addition, a fully non-ergodic approach that separates the epistemic contribution (i.e., the epistemic uncertainty affecting the soil properties) from the total variability in site amplification is presented. To fulfill the scope of the work, the study focuses on three test sites in Italy characterized by different geological conditions and seismicity levels: Mirandola and Soncino in the Po Plain (northern Italy) and Peglio in central Italy.

Introduction

As it is well known, the severity and frequency content of the ground shaking at a site are significantly dependent on the soil characteristics and local geomorphological features (e.g., Stone et al., 1987; Seed et al., 1990; Ameri et al., 2009; Bradley, 2012; Massa et al., 2014). It follows that neglecting site response may result in a severe underestimation of the local ground motion hazard. Therefore, probabilistic seismic hazard analysis (PSHA) based on the assumptions of level ground and exposed bedrock defines only a basic level for the definition of the expected ground motion.

1

Nowadays, in-depth assessments which account for local soil conditions would be advisable, not only for the design of critical facilities (e.g., dams, oil and gas pipelines, nuclear power plants) but also to define updated anti-seismic norms and risk mitigation strategies. Besides studies for critical facilities, where the integration of site-effects into a PSHA has become a standard practice (e.g., Abrahamson et al., 2004; Rodriguez-Marek et al., 2014), detailed hazard mapping inclusive of site-effects is nowadays possible in many regions of the world where extensive seismic microzonation studies have been carrying out, leading to large-scale evaluations of seismic amplification effects.

Various approaches to incorporate the site response into a PSHA, along with case studies and applications, can be found in the scientific literature (e.g., Costantino et al., 1993; Petersen et al., 1997; Field and the SCEC Phase III Working Group, 2000; Romeo, 2000; McGuire, 2001a and 2001b; Cramer, 2003 and 2005; Bazzurro and Cornell, 2004a and 2004b; Pelli et al., 2004; Pelli et al., 2006; Barani et al., 2014a-b; Rodriguez-Marek et al., 2014; Faccioli et al., 2015). The aim of this work is to highlight strengths and weaknesses of a set of procedures for site-specific PSHA (Table 1), including both straightforward but less rigorous approaches and complex probabilistic methods. Rigorously speaking, the term "site-specific hazard", which is extensively used in the article as an alternative to "soil hazard" (as used by Abrahamson et al. (2004)), should be properly used only whether site amplification is quantified via specific ground response analysis at the site of interest. The simplest approach (Level 0) consists of multiplying a hazard curve for reference rock conditions (i.e., an acceleration value corresponding to a mean annual rate of exceedance) by a frequency-independent amplification factor derived from anti-seismic norms (or, occasionally, from ground response analyses). Although it is somewhat employed due to its simplicity, this approach cannot be considered as a rigorous probabilistic method. It produces surface ground-motion levels whose exceedance rates are unknown. Moreover, it ignores site-specific information (Bazzurro and Cornell, 2004b). The more complex method (Level 3) calculates the hazard at the ground surface by combining in a probabilistically robust way the rock-hazard curve at the site of interest with the probability distribution of a frequency-dependent amplification factor obtained from numerical soil

response analyses. In between, one may adopt a ground motion prediction equation (GMPE) calibrated for a specific ground type (Level 1) or modify a rock GMPE by including a site-specific amplification factor determined from numerical simulations (Level 2). This latter method was developed and refined within the framework of the S2-Project to incorporate the results of regional microzonation studies in Italy. As with many European anti-seismic standards (e.g., Comitè Europèen de Normalisation – CEN, 2004), site amplification is quantified by means of frequency-independent amplification factors. Hence, this approach can be viewed as the probabilistic site-specific variation of the Level 0 method. Although the use of such factors does not allow for an accurate definition of site amplification, as they explicitly do not capture differential site amplification effects in different period ranges, this approach may be useful to provide fully probabilistic representations of seismic soil hazard at large scale. We will get into specifics of each method in the next sections, with particular focus on the Level 2 and Level 3 approaches. We specify just now that, with the exception of the ground motion attenuation model, the same input parameters and models adopted by Barani et al. (2009) for the disaggregation of the Italian ground motion hazard (Stucchi et al., 2011) are used in this study to assess the hazard. The GMPE of Ambraseys et al. (1996) has been replaced by the more recent model of Bindi et al. (2011), which is specifically defined for applications in Italy. Note that if site amplification is quantified with respect to a reference soil condition (i.e., rock) that is different from the one used by the GMPEs selected for the PSHA, then those GMPEs should be adjusted to the rock conditions of the target site (e.g., Cotton et al., 2006; Biro and Renault, 2012; Al Atik et al., 2014; Rodriguez-Marek et al., 2014).

To fulfill the scope of the work, three test sites characterized by different geological conditions and seismicity levels have been considered. Two of them, Mirandola and Soncino, which were struck by the May-June 2012 Emilia seismic sequence with main shock of magnitude $M_w = 6.1$ (e.g., Luzi et al., 2013), are located in the Po Plain (northern Italy). The third site, Peglio, is located in central Italy. For all sites, hazard calculations (of Level 2 and Level 3) are performed by removing the ergodic hypothesis, which is conventionally assumed in standard PSHA. In simple words,

3

conventional PSHAs assume that the ground motion variability (sigma) related to a given GMPE calibrated from a large data set of ground motions from various earthquakes recorded at multiple stations is an unbiased estimate of the variability at a single site (e.g., Anderson and Brune, 1999; Al Atik et al., 2010; Rodriguez-Marek et al., 2011). Repeatable and systematic effects of path and source and the effects of the same soil conditions should in general make the ground-motion variability at a single site smaller than that computed using records from other sites affected by other earthquakes with different paths and sources. Hence, part of the variability in the ground motion can be transferred into the epistemic uncertainty affecting the site behavior. Separating the repeatable components of the ground motion variability at a site from the total ground motion variability (ergodic sigma) has the benefit of reducing the ergodic standard deviation by introducing the use of the single-station sigma in place of the ergodic counterpart. The single-station sigma σ_{SS} is given by:

$$\sigma_{SS} = \sqrt{\tau^2 + \phi_{SS}^2} \qquad (1)$$

where τ and ϕ_{SS} are the between-event and event-corrected single-station standard deviations, respectively. The values of ϕ_{SS} used in this study are those determined by Luzi et al. (2014) using the Bindi et al. (2011) ground motion dataset.

However, the removal of the ergodic assumption is paid at a steep price since it implies incorporation of the epistemic uncertainty relative to the site amplification into the PSHA via logic tree (e.g., Rodriguez-Marek et al., 2014). This topic is given particular attention in the section concerning the Level 3 approach. This approach lumps all of the site response uncertainty/variability into aleatory variability rather than separating the epistemic and aleatoric components. We will show how to separate the epistemic contribution from the total standard error related to the (logarithmic) site amplification term, which reflects both the uncertainty in the soil characteristics and the variability of the input ground motion used in the numerical ground response analyses.

A note on ground response analyses

Both the Level 2 and 3 approaches require site-specific ground response analyses to quantify the level of ground motion amplification (or de-amplification) related to local geology. For all 3 sites considered, 1D numerical soil models (Table 2) were defined based on available geotechnical and geophysical data. The uncertainty affecting soil parameter estimates is introduced in the calculations via a Monte Carlo simulation procedure that consists of randomly varying unit weight, shear wave velocity (V_S), shear modulus degradation curve, and damping curve. The uncertainty associated with model geometry was also considered by randomizing the thickness of each soil layer. Two hundred Monte Carlo simulations were performed in this study. Interested readers may found a detailed description of the simulation procedure in the articles of Bazzurro and Cornell (2004a) and Barani et al. (2013). In this latter article, an exhaustive discussion about the importance of modeling the uncertainties affecting soil models is presented. As an example, Figure 1 shows the variability of V_S along each soil profile presented in Table 2. The variability of the modulus reduction and damping curves adopted in the numerical simulations for the sites of Mirandola and Soncino can be appreciated in the annex 6 of the deliverable of the 2012 S2-Project (Task 4 Working Group, 2013).

Numerical ground response analyses were performed using Shake91 (Idriss and Sun, 1993), which implements an equivalent linear approach to model the nonlinear response of soils. The seismic excitation for the numerical ground response analyses, which is here represented by groups of 20 real accelerograms recorded on rock (the list of recordings used in the ground response analyses can be found in the deliverable cited above), was defined in order to be consistent with the magnitude-distance (*M-R*) pairs controlling the peak ground acceleration (PGA) and 1s spectral acceleration ($S_a(f)$ where f denotes the frequency of a 5%-damped oscillator) hazard. According to Bazzurro and Cornell (2004a), special care was taken to select both near-source and far-field records, thus to cover a broad range of magnitude and (epicentral) distance values as well as to include time histories representative of different hazard levels (e.g., acceleration levels corresponding to a mean

return period, MRP, of 50 to 2500 years). This allows the influence of both strong and weak motions on ground response results to be effectively evaluated. In other words, we took care of selecting groups of time histories that span a range of variability related to the input motion. For all sites, Figure 2 shows the magnitude-distance distributions of the selected records and the relative 5%-damped acceleration response spectra. Note that the selected time histories were not scaled to a specific acceleration value (e.g., local PGA corresponding to a given MRP), thus not to alter natural recordings. Moreover, this prevents an undue or artificial reduction of the aleatory variability related to the input motion, which would affect the final hazard estimates at the ground surface.

The results of the ground response analyses are presented Figure 3. For each of the three sites investigated, the figure shows the variability in the soil amplification $AF(f)$, which is here quantified by the ratio of the spectral acceleration at the surface, $S_a^S(f)$, to the spectral acceleration at the base-rock level, $S_a^R(f)$ (Bazzurro and Cornell, 2004a).

Level 2 site-specific PSHA

The Level 2 approach consists of correcting a GMPE for rock conditions by a frequency-independent site-specific amplification factor, F_s, which is defined as the ratio of the response spectrum intensity for 5% damping at the surface, SI^S, to the response spectrum intensity at rock outcrop, SI^R (e.g., Pergalani et al., 1999; Rey et al., 2002; Pergalani et al., 2003; Barani et al., 2008; Gruppo di Lavoro MS, 2008):

$$F_s = \frac{SI^S}{SI^R} \qquad (2)$$

The response spectrum intensity can be simply calculated as:

$$SI = \int_{T_1}^{T_2} Y(T)dT \qquad (3)$$

where $Y(T)$ indicates either the acceleration or pseudo-velocity response spectrum, and $[T_1,T_2]$ represents the range of periods over which the response spectrum is integrated. The pseudo-velocity

response spectrum intensity (Housner, 1952) was recommended for the evaluation of the response of structures and flexible slopes with fundamental periods between 0.6 and 2s while the acceleration spectrum intensity (Von Thun et al., 1988) for analyses of structures with fundamental periods of less than 0.5s (e.g., Makdisi and Seed, 1978; Bray, 2007; Barani et al., 2010). Such parameters, which have large application in slope displacement hazard analysis (e.g., Bray, 2007; Barani et al., 2010), are extensively used in regional microzonation studies in Italy for the definition of F_s. Hence, maps of F_s may be coupled with PSHA to producing large-scale soil hazard scenarios.

In this study, three different amplification factors are computed. One ($F_s = F_a$) covers the same range of periods considered by Rey et al. (2002) for the derivation of the design soil coefficients for the Eurocode 8 provisions (Comitè Europèen de Normalisation – CEN, 2004). Specifically, SI is calculated as the area under the acceleration response spectrum between periods of $T_1 = 0.05$ and $T_2 = 2.5s$. The remaining two, which must be applied in conjunction, allow distinction between short and long spectral periods. At short periods ($\leq 0.5s$), the amplification factor ($F_s = C_a$) is defined as the ratio of the surface-level to the rock-level acceleration spectrum intensities calculated in the spectral range $[T_1, T_2] = [0.01s, 0.5s]$. At longer periods ($> 0.5s$), the amplification factor ($F_s = C_v$) is again calculated using Equation 2 but the acceleration spectrum intensity is replaced by the pseudo-velocity spectrum intensity. The latter parameter is calculated by integration of the pseudo-velocity response spectrum over the range $[T_1, T_2] = [0.4s, 2s]$. The domains of integration used to define C_a and C_v are the same as those used by Borcherdt (1994), with the exception of the lower limit at low periods, which is extended down to 0.01s. For each site investigated, the average values of F_s (μ_{F_s}) and its standard deviation (σ_{F_s}) are presented in Table 3.

Soil amplification can be incorporated into PSHA by modifying an existing rock attenuation model. In logarithmic terms, the mean value of the surface spectral acceleration $S_a^S(T)$ (i.e., the mean of $\ln S_a^S(T)$) at an oscillator period T is calculated as:

$$\ln S_a^S(T) = \ln S_a^R(T) + \ln F_s \quad (4)$$

Numerous analytical expressions for $S_a^R(T)$ in terms of magnitude, distance, and other parameters θ (e.g., source mechanism, soil conditions) have been proposed in the literature. Such attenuation models have typically the following form:

$$\ln S_a^R(T) = g(M, R, \theta) + \varepsilon_{\ln S_a^R(T)} \qquad (5)$$

where $\varepsilon_{\ln S_a^R(T)}$ is the Gaussian residual with zero mean and standard deviation $\sigma_{\ln S_a^R(T)}$. As stated above, the GMPE of Bindi et al. (2011) is applied in this study.

The total standard error of the logarithmic ground motion at the ground surface is given by the following equation which, similarly to Equation 15 in Bazzurro and Cornell (2004b), conservatively neglects potential negative correlations between the spectral acceleration on rock and soil amplification:

$$\sigma_{\ln S_a^S(T)} = \sqrt{\sigma_{\ln S_a^R(T)}^2 + \sigma_{\ln F_S}^2} \qquad (6)$$

where $\sigma_{\ln S_a^R(T)}$ is replaced by σ_{SS} (see Equation 1) if the ergodic assumption is relaxed and $\sigma_{\ln F_S}$ is the standard deviation of $\ln F_s$. Assuming that soil amplification follows a log-normal distribution (Bazzurro and Cornell, 2004a), $\sigma_{\ln F_S}$ can be computed as (e.g., Benjamin and Cornell, 1970):

$$\sigma_{\ln F_S} = \sqrt{\ln(1 + (\sigma_{F_S}/\mu_{F_S})^2)} \qquad (7)$$

where μ_{F_S} and σ_{F_S} are determined from ground response analysis.

Note that Equations 4-7 still hold in the case of frequency-dependent amplification factors.

Figure 4 compares the hazard results, here expressed in terms of uniform hazard spectra (UHSs) corresponding to an MRP of 475 years, obtained by application of the amplification factors listed in Table 3. At Mirandola and Soncino, the distinction between short- and long-period amplification does not produce significant differences in the results. The major differences can be observed at 0.15s where the values of spectral acceleration differ by less than 10%. Despite these small differences, distinction between short- and long-period amplification allows roughly capturing of the frequency-dependence of site amplification. Indeed, while at Mirandola most of amplification

occurs below 4Hz (see Figure 3a), at Soncino it is concentrated towards higher frequencies (> 5Hz; see Figure 3b). This is more evident at the site of Peglio where the use of amplification factors for different spectral ranges leads to a higher hazard in the frequency range 2-12Hz (i.e., $\approx$ 0.08-0.5s), range where major soil amplification effects are observed (see Figure 3c). In this range, differences in the spectral accelerations reach up to approximately 20%.

Removal of ergodicity in Level 3 site-specific PSHA

This approach (Bazzurro and Cornell, 2004b), which is referred to as Approach 3 in the U.S. nuclear industry (McGuire et al., 2001a), computes the surface hazard curve by convolving the reference rock hazard curve with the probability density function of $AF(f)$. Analytical models for $AF(f)$ (hereinafter, soil amplification functions – SAFs) can be determined by regression of $AF(f)$ versus $S_a^R(f)$. The (log-) regression model adopted in this study is represented by the following equation (Bazzurro and Cornell, 2004a):

$$\ln AF(f) = c_1 + c_2 \ln S_a^R(f) + c_3 \left[\ln S_a^R(f)\right]^2 + \varepsilon_{\ln AF(f)} \qquad (8)$$

where $\varepsilon_{\ln AF(f)}$ is the Gaussian residual with zero mean and standard deviation $\sigma_{\ln AF(f)}$.

As with the Level 2 approach, this method fully preserves the probabilities associated with the rock ground motions and transfers these to the surface level. Moreover, it has the advantage to account for site effects frequency by frequency.

In addition to this approach, Bazzurro and Cornell (2004b) have proposed a simplified procedure that integrates a linear predictive model in $\ln S_a^R(f)$ directly into the rock attenuation equation used in the hazard analysis, thus transforming it into a site-specific GMPE. Both the convolution-based approach and the simplified one (Level 3 PSHA with site-specific GMPE) are applied in this study. This section is not intended to present a detailed description of the Level 3 approach but focuses on the decomposition of $\sigma_{\ln AF(f)}$ in its epistemic and aleatoric components. Besides the original article

of Bazzurro and Cornell (2004b), an exhaustive description of this method can be found in the articles of Barani et al. (2014a) and Rodriguez-Marek et al. (2014).

As observed previously, numerical ground response analyses for site-specific PSHA allow for the record-to-record variability of the input excitation as well as for the uncertainty in the soil model, which will be reflected in the standard error of ln$AF(f)$ (i.e., in the probability density function of $AF(f)$). Generally, a single SAF is derived from a set of n Monte Carlo realizations and a group of k accelerograms driven at the base of each random soil model (Figure 5a). Hence, $\sigma_{\ln AF(f)}$ incorporates both the input motion variability and the uncertainty in the soil model parameters. While the former has a pure aleatoric nature (no one knows what strong earthquakes will strike the site under study in the future), the latter is mainly epistemic (since it is related to the lack of knowledge about soil stratigraphy and soil parameter values; e.g., different geophysical methods may lead to alternative V_S profiles), although it is treated as aleatoric through Monte Carlo randomization. Following this approach (here termed as single-SAF Level 3 approach), $\sigma_{\ln AF(f)}$ is therefore ergodic. In order to separate the contribution of the epistemic uncertainty in the soil characteristics from the aleatory variability in the input motion, a SAF (and its related sigma) has to be determined via regression for each one of the n soil samples at the base of which k accelerograms are driven (Figure 5b). This can be done iteratively without much effort. Each SAF and its related aleatory sigma will be then used in the convolution with the rock hazard curve, leading to a bundle of site-specific hazard curves (Figure 6). This approach (here termed as multi-SAF Level 3 approach) can be similarly extended to the Level 2 PSHA. In that case, an F_s, along with its standard deviation, will be determined for each soil sample subjected to a set of input ground motions. This method is again referred to as multi-SAF (Level 2) approach, where SAF stands here for soil amplification factor instead of soil amplification function.

The advantage of the multi-SAF analysis is clearly twofold. On the one hand, it allows distinction between the aleatoric and epistemic components of site amplification. Consequently, it allows direct incorporation of the epistemic uncertainty relative to site response into PSHA as required by the

10

single-station sigma non-ergodic approach. Note that if alternative methods for site response assessment (e.g., fully nonlinear, equivalent linear) are employed in order to account for potential modeling errors, a multi-SAF analysis should be repeated for each of them. Each method should be assigned a subjective weight, which represents the relative likelihood of that method being correct. Conversely, there is no need to assign weights to the randomized soil models. In fact, they are implicitly assigned within the framework of the Monte Carlo simulation when a probability density function is selected for each uncertain property. For instance, if a random variable is drawn from a Gaussian distribution with specified mean and standard deviation, the majority of realizations of the random process will be concentrated around the mean, in agreement with the probability density function chosen, and only few extreme (low likelihood) values will be sampled.

Figure 7 compares the UHSs (again for an MRP of 475 years) assessed by applying three alternative variations of the Level 3 approach. One modifies the Bindi et al. (2011) rock GMPE by integrating an analytical linear expression of $AF(f)$ directly into the original model. One is based on the single-SAF convolution procedure. One is the multi-SAF approach defined herein. Comparing the UHSs resulting from the latter two approaches does not reveal substantial differences in the spectral acceleration hazard values. However, as in the case of Peglio (Figure 7c), removing the epistemic uncertainty related to the soil properties from $\sigma_{\ln AF(f)}$ may have the appreciable benefit of slightly lowering (by an amount of less than 12% in this example) the mean hazard. Compared to this latter approach, the one based on the site-specific version of the Bindi et al. (2011) GMPE is found to lead to very similar hazard results, subject to the condition that a linear predictive model of $AF(f)$ in terms $S_a^R(f)$ is appropriate. For instance, for the case study of Mirandola, the values of the spectral acceleration at the ground surface for an MRP of 475 years are always lower than those assessed via both the single- and multi-SAF approaches, which use a quadratic model in $\ln S_a^R(f)$ (Equation 8) instead. As indicated by the values of the coefficient of multiple determination (R^2), this is attributable to the lower predictive power of the linear models for $AF(f)$ incorporated into

the GMPE used in the calculations, particularly at low-to-intermediate periods where certain strong motion records used in the numerical simulations were found to induce some soil nonlinearity.

Comparison of Level 0-to-Level 3 hazard estimates

Figure 8 summarizes the results of this work by comparing the UHSs assessed for an MRP of 475 years by applying each one of the Level 0-to-Level 3 approaches for the three test sites under study. The results for an MRP of 2475 years are shown in Figure 9. The values of the site factors (S_S) employed in the Level 0 assessment are provided in Table 3. Concerning the Level 2 and Level 3 results, the figures show the mean UHSs resulting from the application of the fully non-ergodic multi-SAF approach presented in this research. The relevant uncertainty bands delimited by the 2nd and 98th percentile UHSs are also displayed. Distinction between short- and long-period amplification is made in the case of the Level 2 PSHA. Focusing on an MRP of 475 years and on the test sites in the Po Plain (Mirandola and Soncino), the Level 1 approach provides the highest spectral acceleration hazard in almost the whole spectral range considered (Figure 8a and 8b). Compared to the 475-yr Level 3 mean spectral accelerations, which are here considered as reference, the Level 1 estimates can be as high as a factor of 1.7 (at 0.1s) at Mirandola and 2.2 (at 2s) at Soncino. At this latter site, the Level 0 UHS, which however can not be considered as strictly probabilistic (hence, the definition of "uniform hazard spectrum" is used improperly), approximates fairly well the Level 3 average UHS, particularly below 0.2s where the spectral acceleration values are just a bit more conservative. At Mirandola, Level 1 estimates are over-conservative below 0.25s (exceeding the upper limit of the uncertainty band relative to the Level 3 hazard), under-conservative between 0.25s and 0.7s, and nearly coincident at longer periods. A similar trend is shown by the Level 2 UHS which, compared to the Level 1 one, provides lower hazard values below 0.2s. In this range, the Level 2 average spectral accelerations are close to the 98% percentile UHS obtained using the Level 3 approach. At Soncino, the Level 2 UHS follows closely the Level 3 spectrum with the only exception of the acceleration values in the 0.1-0.15s spectral range where

soil resonance occurs (see Figure 3b). In this range, the 475-yr Level 3 average ground motions are approximately 15% greater than those assessed by the Level 2 approach which, due to the frequency-independence nature of F_s, tends to flatten site effects near the soil resonance frequencies. A similar but less evident behavior can be observed at Peglio in the 0.15-0.3s range (Figure 8c). At this site, the Level 2 mean UHS for an MRP of 475 years assumes greater values between 0.4s and 0.7s while, at longer periods, it is almost coincident with the Level 3 UHS. At these medium-to-long periods (precisely for $T \geq 0.5$s), also the Level 0 estimates are in very good agreement with those provided by the Level 3 approach. The Level 1 approach tends to underestimate the Level 3 average accelerations at short spectral periods (< 0.4s) and to produce significantly higher hazard (up to 1.6-to-1.8 times greater) at longer periods. Analogous observations can be made for an MRP of 2475 years (Figure 9). Compared to an MRP of 475 years, it is worth noting the larger differences between the spectral acceleration values assessed by application of the Level 0-to-Level 2 approaches and those resulting from the Level 3 PSHA at the site of Mirandola. This may be related to soil nonlinearity induced by the strongest ground motion records (whose contribution to the site hazard is known to increase with increasing the MRP (e.g., Bazzurro and Cornell, 1999; Barani et al., 2009)) used in the site response analyses, soil nonlinearity which is only captured by the Level 3 approach.

Conclusions

Previous considerations allow us to conclude the article highlighting advantages and disadvantages of the approaches examined. As expected, all Level 0-to-Level 2 approaches may provide only a basic representation (particularly the Level 0 and Level 1 approaches) of the hazard at a site, in the sense that they might not capture effectively the "actual" ground response at the site of interest. In other words, they may provide hazard results that can be either over-conservative or under-conservative dependently on the period range. Hence, the incorporation of epistemic uncertainties related to soil amplification appears an inseparable component of any soil PSHA, independently of

the level of sophistication of the computational approach selected. In particular, as the degree of sophistication decreases, the epistemic uncertainty should be increasing. Nevertheless, the Level 0 approach has the important drawback that it leads to hazard results that are neither site-specific nor probabilistic. Therefore, although it was found to provide results that match the Level 3 hazard estimates in some period ranges, its use should be discouraged. The Level 1 PSHA produces only a broad, generic assessment of the hazard since it does not account for site-specific information. Therefore, its use should be limited to generic large-scale hazard mapping. Interested readers may refer to the article of Barani et al. (2016) in this journal issue for a statistical analysis aimed at evaluating the feasibility of such method to large-scale hazard assessments in Italy. Unlike the two previous approaches, which strictly speaking can not be considered as site-specific, the Level 2 method accounts for ground response through the incorporation of site-specific amplification factors (e.g., estimated within the framework of microzonation studies) into an existing rock GMPE. However, due to the frequency-independent nature of the site factors, which basically neglect differences in site amplification at different response periods, this approach might not provide fully conservative hazard estimates, especially around the soil resonance frequencies. Therefore, as with the Level 1 approach, its use should be limited to provide an approximate assessment of the soil hazard only at large-scale.

Despite its complexity, which is mainly related to the evaluation of the ground response of the site under study and the subsequent computation of at least an analytical model for $AF(f)$ for each frequency of interest, the Level 3 approach has the strength to capture exhaustively the soil response frequency by frequency, subject to the condition that the real response of the site is accurately represented by the ground response computed by the software at hand. A further strength is that the method decouples the soil hazard computation and the rock hazard assessment. Thus, the soil hazard can be assessed without the need of computing the hazard on rock from scratch; that is, by convolving site-specific soil amplification functions with exiting rock hazard curves. In that case, the existing curves should span over a large range of acceleration values. "*In extreme cases, the*

exceedance of a particular soil-ground-motion level may in fact occur both for a very small bedrock ground motion significantly amplified by the nearly linear soil response or for a large bedrock ground motion greatly de-amplified by the nonlinear behavior of the soil column" (Bazzurro and Cornell, 2004b). The Level 3 approach, as well as the Level 2 one, can be applied within the framework of a fully non-ergodic PSHA that uses single-station sigmas in place of the ergodic ones, with no need of introducing alternative assumptions concerning site response (if the epistemic uncertainty in the soil amplification is exhaustively captured by the Monte Carlo realizations of the soil model and by the method selected for the ground response analysis). As observed above, the epistemic uncertainty in the soil characteristics can be separated from the aleatory variability related to the soil amplification, leading to a set of analytical model for $AF(f)$ for each specified value of f. Each soil amplification function will be then used, along with the hazard curves on rock, in the convolution approach to determine the hazard at the ground surface. Despite its strengths, the Level 3 approach has an important drawback. As with many refined and computationally demanding methods, its use is justifiable if adequate input data are available at all levels, from the selection of the input ground motion to the definition of the soil models. If input data and models are lacking or unreliable, the use of the Level 3 approach appears inappropriate. Thus, this method does not seem to be suitable to large-scale hazard assessments. To overcome this limitation, one could use target soil amplification functions determined for different soil profiles, each one representative of particular soil conditions. Obviously, such an approach requires the implicit assumption that the soil conditions in the study area resemble those at the target sites.

Acknowledgements

References

Abrahamson NA, Coppersmith KJ, Koller M, Roth P, Sprecher C, Toro GR, Youngs R (2004), Probabilistic seismic hazard analysis for Swiss nuclear power plant sites (PEGASOS Project). Final Report, Volume 1. http://www.swissnuclear.ch/upload/cms/user/PEGASOSProjectReportVolume1-new.pdf. Accessed 15 April 2016.

Al Atik L, Abrahamson N, Bommer JJ, Scherbaum F, Cotton F, Kuehn N (2010) The variability of ground-motion prediction models and its components. Seismological Research Letters 81:794-801.

Al Atik L, Kottke A, Abrahamson N, Hollenback J (2014) Kappa (κ) scaling of ground-motion prediction equations using an inverse random vibration theory approach. Bulletin of the Seismological Society of America 104:336-346.

Ambraseys NN, Simpson KA, Bommer JJ (1996) Prediction of horizontal response spectra in Europe. Earthquake Engineering and Structural Dynamics 25:371-400.

Ameri G, Massa M, Bindi D, D'Alema E, Gorini A, Luzi L, Marzorati S, Pacor F, Paolucci R, Puglia R, Smerzini C (2009) The 6 April 2009 Mw 6.3 L'Aquila (Central Italy) earthquake: strong-motion observations. Seismological Research Letters 80:951-966.

Anderson JG, Brune J (1999) Probabilistic seismic hazard analysis without the ergodic assumption. Seismological Research Letters 70:19-28.

Barani S, Albarello D, Spallarossa D, Massa M (2016) Empirical scoring of ground motion prediction equations for probabilistic seismic hazard analysis in Italy including site effects. Bulletin of Earthquake Engineering, this issue, under review.

Barani S, De Ferrari R, Ferretti G, Eva C (2008) Assessing the effectiveness of soil parameters for ground response characterization and soil classification. Earthquake Spectra 24:565:597.

Barani S, Spallarossa D, Bazzurro P (2009) Disaggregation of probabilistic ground-motion hazard in Italy. Bulletin of the Seismological Society of America 99:2638-2661.

Barani S, Spallarossa D, Bazzurro P, Pelli F (2014a) The multiple facets of probabilistic seismic hazard analysis: a review of probabilistic approaches to the assessment of different hazards caused by earthquakes. Bollettino di Geofisica Teorica e Applicata 55:17-40.

Barani S, Massa M, Lovati S, Spallarossa D (2014b) Effects of surface topography on ground shaking prediction: implications for seismic hazard analysis and recommendations for seismic design. Geophysical Journal International 197:1551-1565.

Barani S, Bazzurro P, Pelli F (2010) A probabilistic method for the prediction of earthquake-induced slope displacements. In: Proceedings of the Fifth International Conference on Recent Advances in Geotechnical Earthquake Engineering and Soil Dynamics, May 24-29, San Diego, California, Paper No 4.31b.

Barani S, De Ferrari R, Ferretti G (2013) Influence of soil modeling uncertainties on site response. Earthquake Spectra 29:705-732.

Bazzurro P, Cornell CA (1999) Disaggregation of seismic hazard. Bulletin of the Seismological Society of America 89:501-520.

Bazzurro P, Cornell CA (2004a) Ground-motion amplification in nonlinear soil sites with uncertain properties. Bulletin of the Seismological Society of America 94:2090-2109.

Bazzurro P, Cornell CA (2004b) Nonlinear soil-site effects in probabilistic seismic-hazard analysis. Bulletin of the Seismological Society of America 94:2110-2123.

Benjamin JR and Cornell CA (1970) Probability, statistics, and decision for civil engineers. McGraw-Hill, New York.

Bindi D, Pacor F, Luzi L, Puglia R, Massa M, Ameri G, Paolucci R (2011) Ground motion prediction equations derived from the Italian strong motion database. Bulletin of Earthquake Engineering 9:1899-1920.

Biro Y, Renault P (2012) Importance and impact of host-to-target conversions for ground motion prediction equations in PSHA. In: Proceedings of the 15th World Conference on Earthquake Engineering, September 24-28, Lisbon, Portugal, Paper No 1855.

Boore DM, Joyner WB (1983) Ground motions and response spectra at soil sites from seismological models of radiated spectra. U.S. Geological Survey Open-File Report 83-845, 261-279.

Borcherdt RD (1994) Estimates of site-dependent response spectra for design (methodology and justification). Earthquake Spectra 10:617-653.

Bradley BA (2012) Strong ground motion characteristics observed in the 4 September 2010 Darfield, New Zealand earthquake. Soil Dynamics and Earthquake Engineering 42:32-46.

Bray JD (2007) Simplified slope displacement procedures. In: Pitilakis KD (ed) Earthquake Geotechnical Engineering, pp 327-353.

Bray JD (2007) Simplified slope displacement procedures. In: Pitilakis KD (ed) Earthquake Geotechnical Engineering, Springer, Dordrecht, Netherlands, pp. 327-353.

Comitè Europèen de Normalisation (2004) Eurocode 8: Design of structures for earthquake resistance, Part 1: General rules, seismic actions and rules for buildings. Brussels, Belgium.

Costantino CJ, Miller CA, Heymsfield E (1993) Site specific seismic hazard calculations at deep soil sites. In: Proceedings of the 4th U.S. Department of Energy Natural Phenomena Hazards Mitigation Conf., LLNL CONF-9310102, pp. 199-205.

Cotton F, Scherbaum F, Bommer JJ, Bungum H (2006) Criteria for selecting and adjusting ground-motion models for specific target regions: application to central Europe and rock sites. Journal of Seismology 10:137-156.

Cramer CH (2003) Site-specific seismic-hazard analysis that is completely probabilistic. Bulletin of the Seismological Society of America 93:1841-1846.

Cramer CH (2005) Site-specific seismic-hazard analysis that is completely probabilistic, Erratum. Bulletin of the Seismological Society of America 95:2026.

Faccioli E, Paolucci R, Vanini M (2015) Evaluation of probabilistic site-specific seismic-hazard methods and associated uncertainties, with applications in the Po Plain, Northern Italy. Bulletin of the Seismological Society of America 105:2787-2807.

Field EH and the SCEC Phase III Working Group (2000) Accounting for site effects in probabilistic seismic hazard analyses of southern California: overview of the SCEC phase III report. Bulletin of the Seismological Society of America 90:1-31.

Gruppo di lavoro MS (2008) Indirizzi e criteri per la microzonazione sismica. Conferenza delle Regioni e delle Province autonome - Dipartimento della protezione civile, Roma, 3 vol. e Dvd. http://www.protezionecivile.gov.it/jcms/it/view_pub.wp?contentId=PUB1137. Accessed 27 April 2016.

Housner GW (1952) Spectrum intensities of strong motion earthquakes. In: Proceedings of the Symposium on Earthquake and Blast Effects on Structures, EERI, Oakland, California, USA, pp. 20-36.

Idriss IM, Sun JI (1993) User's manual for Shake91: A computer program for conducting equivalent linear seismic response analyses of horizontally layered soil deposit. Center for geotechnical modeling, Dept. of Civil and Environmental Engineering, University of California, Davis.

Luzi L, Bindi D, Puglia R, Pacor F, Oth A (2014) Single-station sigma for Italian strong-motion stations. Bulletin of the Seismological Society of America 104:467-483.

Luzi L, Pacor F, Ameri G, Puglia R, Burrato P, Massa M, Augliera P, Castro R, Franceschina G, Lovati S (2013) Overview on the strong motion data recorded during the May-June 2012 Emilia seismic sequence. Seismological Research Letters 84:629-644.

Makdisi FI, Seed H.B. (1978) Simplified procedure for estimating dam and embankment earthquake-induced deformations. Journal of the Geotechnical Engineering Division, ASCEE, No. 104, 849-867.

Massa M, Barani S, Lovati S (2014) Overview of topographic effects based on experimental observations: meaning, causes and possible interpretations. Geophysical Journal International 197:1537-1550.

McGuire RK, Silva WJ, Costantino CJ (2001a) Technical basis for revision of regulatory guidance on design ground motions: development of hazard- and risk-consistent spectra for two sites. Report NUREG/CR-6769, U.S. Nuclear Regulatory Commission, Washington D.C.

McGuire RK, Silva WJ, Kenneally R (2001b) New design spectra for nuclear power plants. Nuclear Engineering and Design 203:249-257.

Ministero delle Infrastrutture e dei Trasporti (2008) Norme tecniche per le costruzioni. D.M. 14 Gennaio 2008, Supplemento ordinario alla Gazzetta Ufficiale No. 29, 4 Febbraio 2008.

Pelli F, Mangini M, Bazzurro P, Eva C, Spallarossa D, Barani S (2006) PSHA in northern Italy accounting for non-linear soil behaviour and epistemic uncertainty. In: Proceedings of the 1st European Conference on Earthquake Engineering and Seismology – ECEES, Geneva, Switzerland, Paper No. 1464.

Pelli F, Bazzurro P., Mangini M., Spallarossa D (2004) Probabilistic seismic hazard mapping with site amplification effects. In: Proceedings of the 11th International Conf. on Soil Dynamics and Earthquake Engineering, Berkeley, California, 7-9 January 2004, Vol. 2, pp. 230-237.

Pergalani F, Compagnoni M, Petrini V (2003) Evaluation of site effects in some localities of 'Alta Val Tiberina Umbra' (Italy) by numerical analysis. Soil Dynamics and Earthquake Engineering 23:85-105.

Pergalani F, Romeo R, Luzi L, Petrini V, Pugliese A, Sanò T (1999) Seismic microzoning of the area struck by Umbria-Marche (Central Italy) Ms 5.9 earthquake of 26 September 1997. Soil Dynamics and Earthquake Engineering 19:279-296.

Petersen MD, Bryant WA, Cramer CH, Reichle MS, Real CR (1997) Seismic ground-motion hazard mapping incorporating site effects for Los Angeles, Orange, and Ventura Counties, California: a geographical information system application. Bulletin of the Seismological Society of America 87:249-255.

Rey J, Faccioli E, Bommer JJ (2002) Derivation of design soil coefficients (S) and response spectral shapes for Eurocode 8 using the European Strong-Motion database. Journal of Seismology 6:547-555.

Rodriguez-Marek A, Montalva GA, Cotton F, Bonilla F (2011) Analysis of single-station standard deviation using the KiK-net data. Bulletin of the Seismological Society of America 101:1242-128.

Rodriguez-Marek A, Rathje EM, Bommer JJ, Scherbaum F, Stafford PJ (2014) Application of single-station sigma and site-response characterization in a probabilistic seismic-hazard analysis for a new nuclear site. Bulletin of the Seismological Society of America 104:1601-1619.

Romeo R, Paciello A, Rinaldis D (2000) Seismic hazard maps of Italy including site effects. Soil Dynamics and Earthquake Engineering 20:85-92.

Seed RB, Dickenson SE, Reimer MF, Bray JD, Sitar N, Mitchell JK, Idriss IM, Kayen RE, Kropp A, Harder LF, Power MS (1990) Preliminary report on the principal geotechnical aspects of the October 17, 1989 Loma Prieta earthquake. Report UCB/EERC-90/05, Earthquake Engineering Reasearch Center, University of California, Berkeley, 137 pp.

Stone WC, Yokel FY, Celebi M, Hanks T, Leyendecker EV (1987) Engineering aspects of the September 19, 1985 Mexico earthquake. NBS Building Science Series 165, National Bureau of Standards, Washington D.C., 207 pp.

Stucchi M, Meletti C, Montaldo V, Crowley H, Calvi GM, Boschi E (2011) Seismic hazard assessment (2003-2009) for the Italian building code. Bulletin of the Seismological Society of America 101:1885-1911.

Task 4 Working Group (2013) D4.1 – Site-specific hazard assessment in priority areas. Deliverable of the DPC-INGV S2 Project "Constraining observations into Seismic Hazard". https://sites.google.com/site/ingvdpc2012progettos2/deliverables/d4-1. Accessed 14 April 2016.

Von Thun JL, Rochim LH, Scott GA, Wilson JA (1988) Earthquake ground motions for design and analysis of dams. In: Earthquake Engineering and Soil Dynamics II – Recent Advance in Ground-Motion Evaluation, Geotechnical Special Publication, No. 20, ASCEE, New York, pp. 463-481.

List of table captions

Table 1 List of probabilistic soil hazard methods.

Table 2 Soil models for the selected sites of Mirandola, Soncino, and Peglio. V_S: shear wave velocity; h: soil thickness; γ: unit weight. The uncertainty affecting each random variable (expressed by its standard deviation) is given in brackets.

Table 3 Average values of site-specific, frequency-independent soil amplification factors (intervals of definition are provided for each factor). The standard deviation of each factor is given in brackets. The values of the soil factor (S_S) defined by the Italian building code (Ministero delle Infrastrutture e dei Trasporti, 2008), which are adopted in the Level 0 computations, are also indicated.

Table 1

Hybrid probabilistic-deterministic	Fully probabilistic		
Level 0	**Level 1**	**Level 2**	**Level 3**
PSHA on rock multiplied by a soil factor derived from anti-seismic norms (or ground response analysis)	PSHA based on GMPEs defined for specific ground types	PSHA based on GMPEs adjusted to incorporate a site-specific frequency-independent amplification factor	PSHA on rock convolved with a site-specific frequency-dependent empirical amplification function

Table 2

		Mirandola	Soncino	Peglio
Layer 1	Material	Clay	Clay	Clay/Marl
	h (σ_h)	12 m (1)	4 m (1)	3 m (*)
	V_S (σ_{V_S})	180 m/s (11)	310 m/s (19)	116 m/s (12)
	γ (σ_γ)	17.5 kN/m³ (1.1)	17.5 kN/m³ (1.1)	16.0 kN/m³ (1.0)
Layer 2	Material	Sand	Gravel	Clay/Marl
	h (σ_h)	18 m (1)	13 m (1)	9 m (*)
	V_S (σ_{V_S})	270 m/s (17)	630 m/s (39)	241 m/s (24)
	γ (σ_γ)	18.2 kN/m³ (1.1)	18.0 kN/m³ (1.1)	17.0 kN/m³ (1.0)
Layer 3	Material	Sand	Rock	Clay/Marl
	h (σ_h)	10 m (1)	∞	19 m (*)
	V_S (σ_{V_S})	475 m/s (30)	930 m/s (58)	571 m/s (57)
	γ (σ_γ)	18.2 kN/m³ (1.1)	19.0 kN/m³ (1.2)	19.0 kN/m³ (1.2)
Layer 4	Material	Sand		Softer rock
	h (σ_h)	25 m (1)		9 m (*)
	V_S (σ_{V_S})	288 m/s (18)		571 m/s (57)
	γ (σ_γ)	18.2 kN/m³ (1.1)		19.0 kN/m³ (1.2)
Layer 5	Material	Sand		Rock
	h (σ_h)	35 m (1)		∞
	V_S (σ_{V_S})	400 m/s (25)		973 m/s (98)
	γ (σ_γ)	18.2 kN/m³ (1.1)		21.5 kN/m³ (1.3)
Layer 6	Material	Softer rock		
	h (σ_h)	20 m (1)		
	V_S (σ_{V_S})	775 m/s (48)		
	γ (σ_γ)	19.1 kN/m³ (1.2)		
Layer 7	Material	Rock		
	h (σ_h)	∞		
	V_S (σ_{V_S})	800 m/s (50)		
	γ (σ_γ)	20.0 kN/m³ (1.2)		

*It is assumed that the uncertainty in the soil thickness increases with depth following a log-normal distribution with $\sigma_{\ln h} = 0.1$

Table 3

Site	F_a (σ_{F_a}) 0.05s $\leq T \leq$ 2.5s	C_a (σ_{C_a}) 0.01s $\leq T \leq$ 0.5s	C_v (σ_{C_v}) 0.4s $\leq T \leq$ 2s	S_S
Mirandola	1.735 (0.257)	1.616 (0.346)	1.968 (0.242)	1.493
Soncino	1.205 (0.139)	1.330 (0.166)	1.044 (0.045)	1.200
Peglio	2.150 (0.608)	2.625 (0.677)	1.450 (0.345)	1.441

List of figure captions

Figure 1 Two hundred shear wave velocity profiles generated via Monte Carlo simulation for the sites of Mirandola (a), Soncino (b), and Peglio (c). Mean V_S profiles (see Table 2) are shown by black curves.

Figure 2 Distributions of the input ground motion records superimposed to the *M-R* contributions to the local PGA hazard corresponding to an MRP of 475 years (top charts) and relative response spectra (bottom charts): (a) Mirandola, (b) Soncino, (c) Peglio. $\overline{M}$ - $\overline{R}$ and M^* - R^* indicate mean and modal magnitude-distance pairs, respectively.

Figure 3 Response spectral ratios, $AF(f)$, resulting from 200 Monte Carlo simulations for Mirandola (a), Soncino (b), and Peglio (c).

Figure 4 Level 2 UHSs for an MRP of 475 years for the sites of Mirandola (a), Soncino (b), and Peglio (c). The UHSs in black account for short- and long-period amplification by means of separate site-specific amplification factors, C_a and C_v, while those in gray use a single site factor, F_a, for the whole spectral band considered.

Figure 5 Ergodic (a) and non-ergodic (b) soil amplification functions (SAFs) relative to a frequency of $f = 10$Hz for the site of Mirandola.
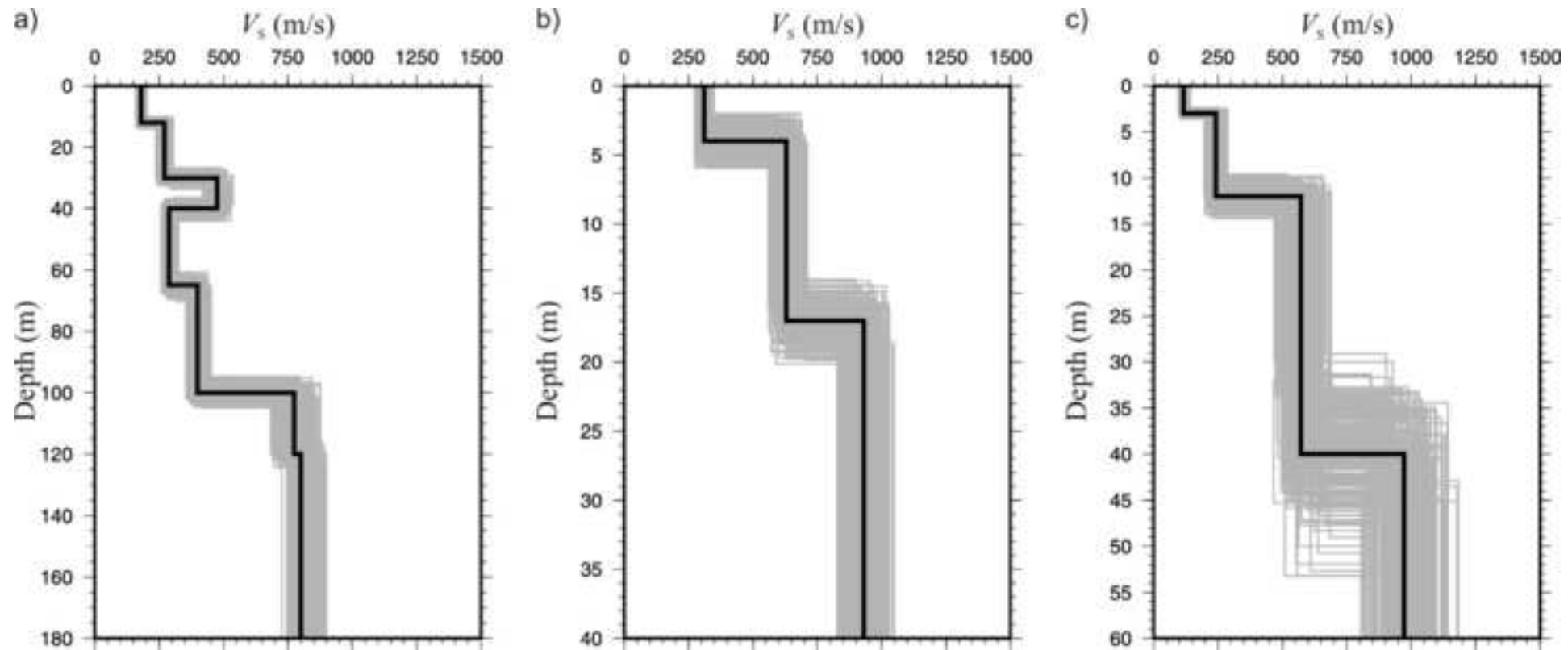
Figure 6 Example of epistemic uncertainty in the site-specific S_a(10Hz) hazard curves of Mirandola due to the uncertainty in the soil model properties. MRE stands for mean annual rate of exceedance.
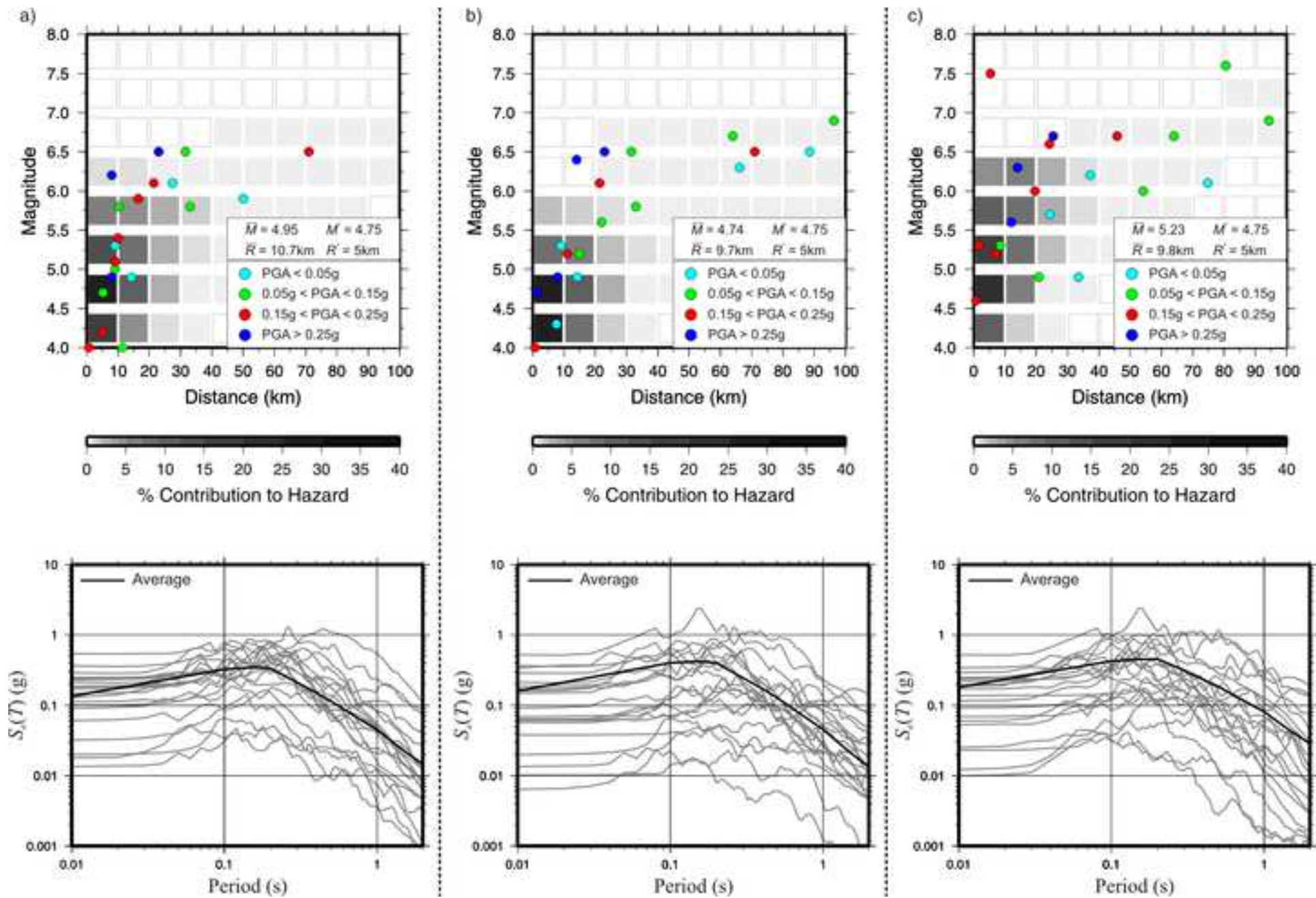
Figure 7 Comparison of Level 3 UHSs for an MRP of 475 years for the three test sites considered: (a) Mirandola, (b) Soncino, and (c) Peglio. The shaded area in gray indicates the uncertainty band between the 2nd and 98th percentile UHSs determined by applying the multi-SAF non-ergodic approach. The mean spectral acceleration hazard is indicated by the UHS in black.
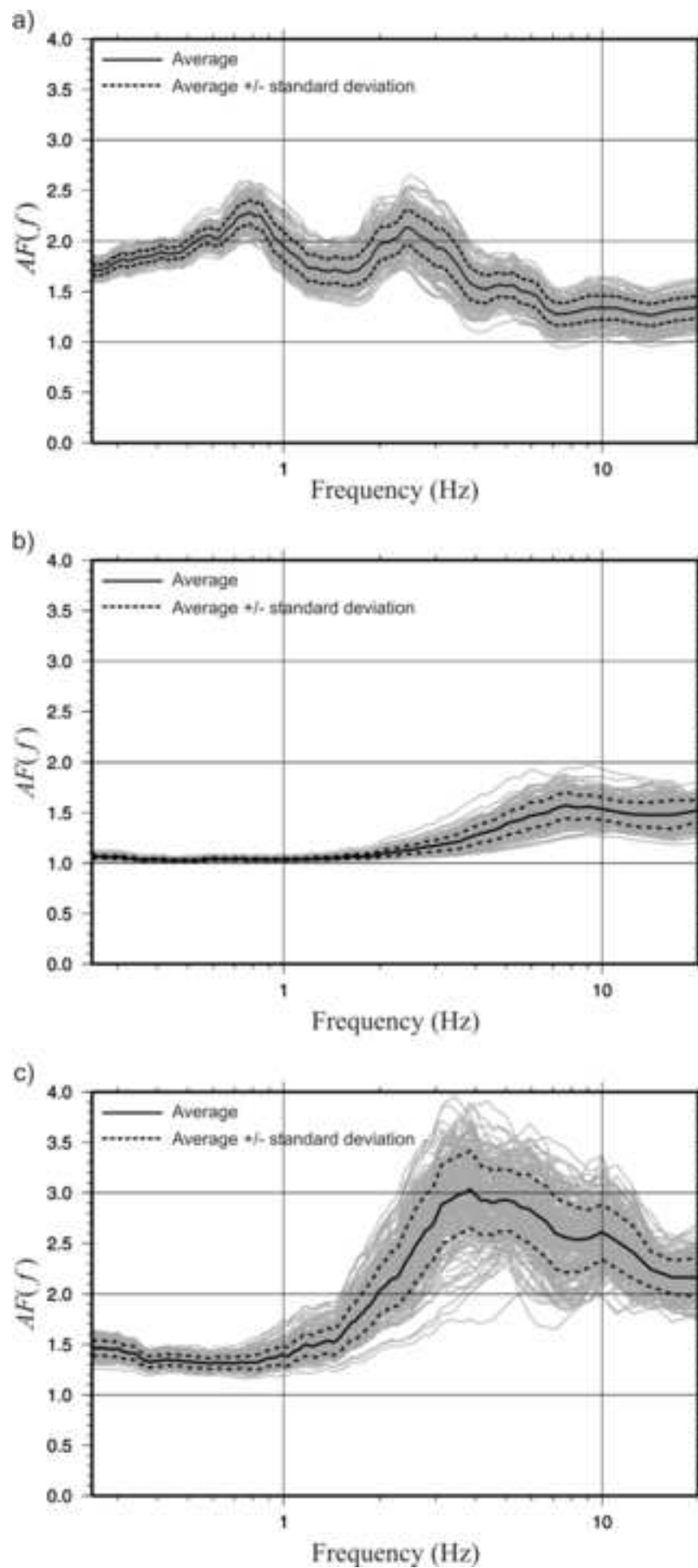
Figure 8 Comparison of Level 0-to-Level 3 UHSs for an MRP of 475 years for the three test sites considered: (a) Mirandola, (b) Soncino, and (c) Peglio. Both multi-SAF Level 2 and Level 3 UHSs are average spectra. The area with the striped pattern and the shaded area in gray indicate the
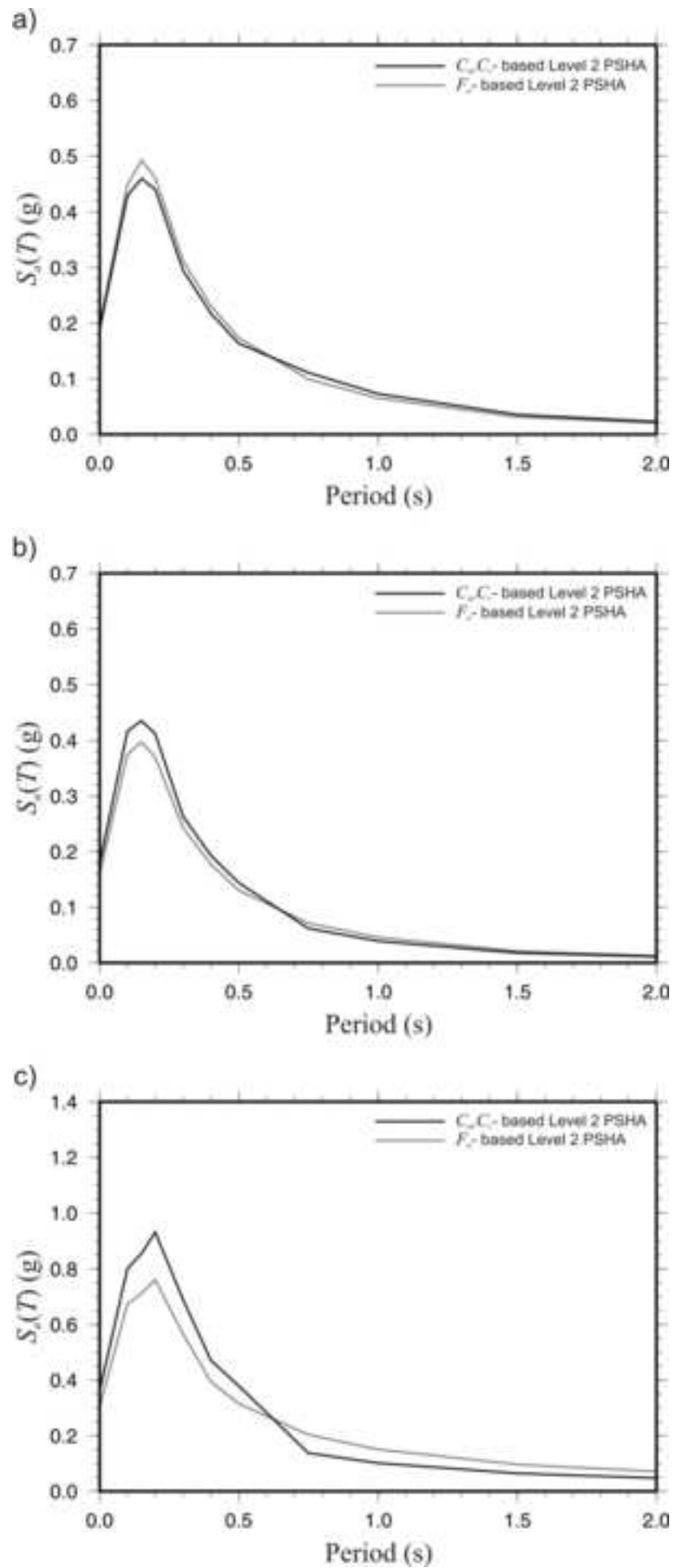
uncertainty bands between the 2nd and 98th percentile UHSs determined by applying the multi-SAF

Level 2 and Level 3 non-ergodic approaches, respectively.

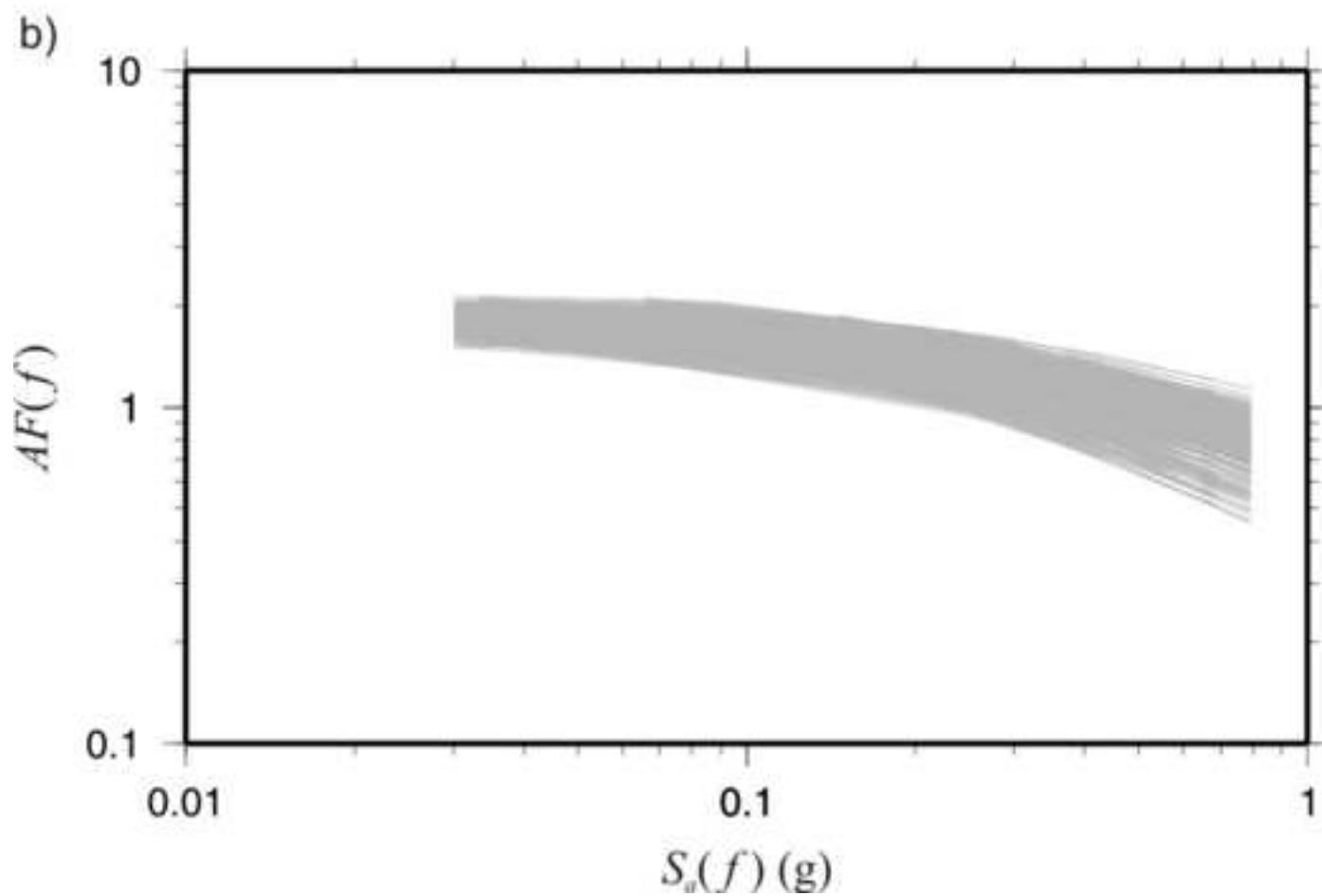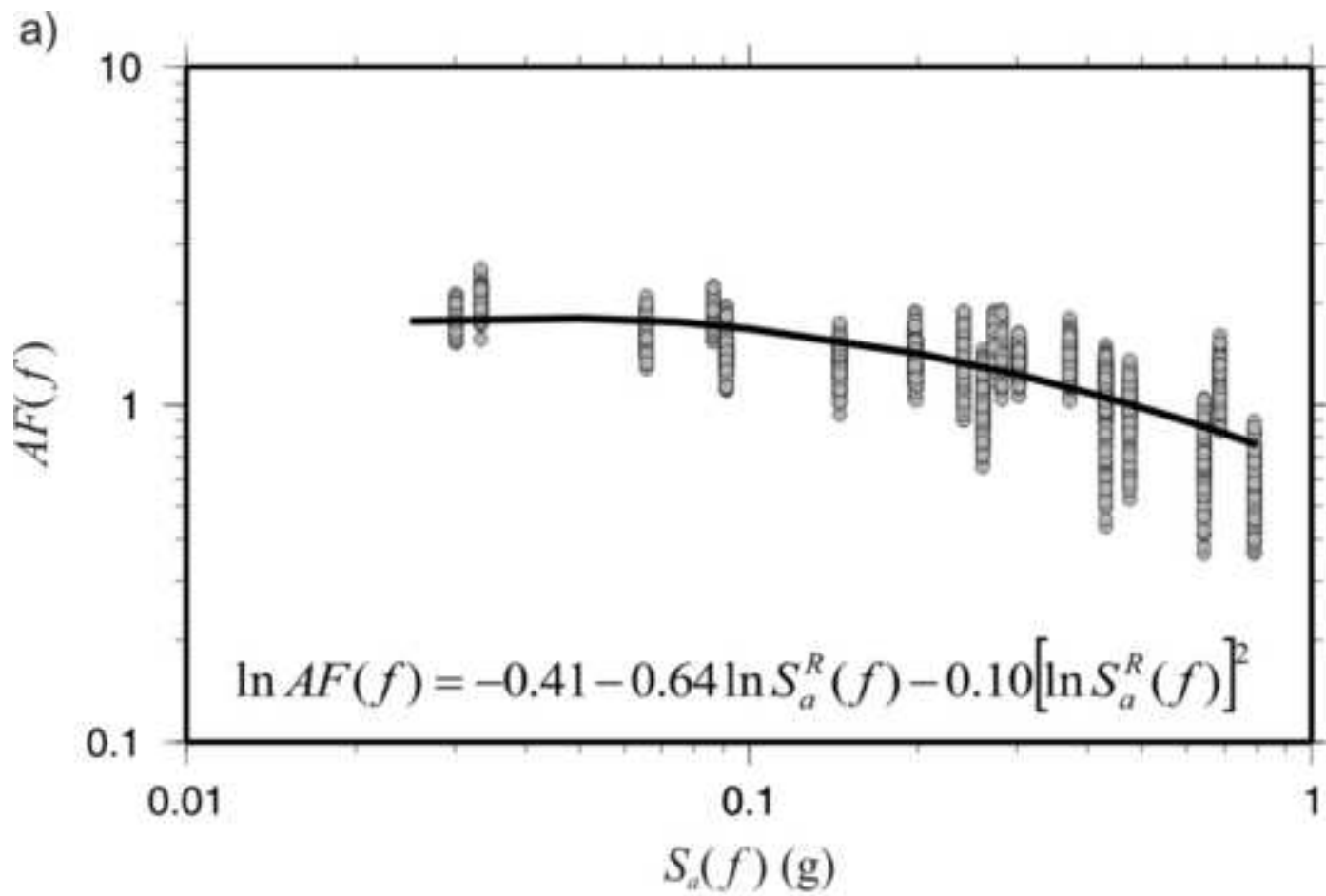**Figure 9** Same as Figure 8 but for an MRP of 2475 years.

Figure 1   Click here to download colour figure Figure1.jpg

Figure 1

Figure 2

Click here to download colour figure Figure2.jpg

Figure 2

Figure 3

Figure 4

Figure 5

a)

$$\ln AF(f) = -0.41 - 0.64 \ln S_a^R(f) - 0.10\left[\ln S_a^R(f)\right]^2$$

AF(f)

$S_a(f)$ (g)

b)

AF(f)

$S_a(f)$ (g)

Figure 6

Figure 7

Figure 7

Figure 8

Figure 8

Figure 9